mater.scichina.com link.springer.com

Published online 26 October 2023 | https://doi.org/10.1007/s40843-023-2652-y
Sci China Mater 2023, 66(11): 4334–4341

SPECIAL TOPIC: High-performance Structural Materials

Dissolution manufacturing strategy for designing tailorable porous glass surfaces

Junsheng Liu, Fei Sun, Xiangyang Yu, Heting Zhang, Jinbiao Huang, Wenxue Wang, Lixing Zhu, Jianan Fu, Wenqing Ruan, Shuai Ren and Jiang Ma*

ABSTRACT **Micro- and nano-structures are a new type of material structures that combines micrometer- and nanometer-scale structures in a single material, which confers special properties on the material. Designing and fabricating micro- and nano-structures on glass surfaces hold great importance for achieving desired functionalities. However, the inherent hardness and brittleness of glass pose challenges for preparing micro-structures using traditional fabrication methods. Thus, developing a simple and controlled manufacturing strategy becomes imperative to prepare micro- and nano-structured glasses with functional applications. In this work, an innovative approach that employed soluble NaCl particles as precursor templates was presented, allowing the formation of customizable porous structures on glass surfaces. Using the pioneering molding strategy proposed here, the potential of soluble NaCl particles as templates was successfully harnessed, thereby facilitating the fabrication of tailorable porous glass surfaces. By tuning the size and combination of these particles, porous glasses ranging from superhydrophilic (1°) to superhydrophobic (142°) were achieved. Notably, the prepared porous glass surfaces demonstrated remarkable lipophilicity, highlighting its great potential for diverse applications, such as oil–water separation and self-cleaning. Importantly, even after undergoing 10 fabrication iterations, the hydrophobic–oleophilic functionality of the glass surface remained intact, underscoring the durability and repeatability of our strategy. This approach offers a convenient and cost-effective means to achieve special functions in glass, paving the way for advancements across various fields.**

Keywords: micro- and nano-porous glass, dissolvable particles, tunable contact angle, reproducible manufacturing

INTRODUCTION

Glass is a very common amorphous solid material that is closely related to our lives and is indispensable in electronics, precision instruments, construction and automobiles [1–4]. Micro- and nano-structures offer various special functionalities to glass, including improved transparency [5], energy storage [6–8], sound isolation [9,10], thermal insulation [11–13], adsorption separation [14–17], catalysis [18–20], and microreactors [21,22]. Recently, porous glass embedded with micro- and nano-structures has attracted substantial attention in industrial and research fields [23,24].

Due to the inherent brittleness of glass, conventional manufacturing methods, such as ultraprecision grinding and milling [25,26], are not particularly suitable for fabricating micro- and nano-structures on glass. Furthermore, specialized techniques, such as laser etching [5,27,28] and focused ion beam [29,30], with their high production cost, are not suitable for a wide range of applications. Meanwhile, inexpensive fabrication methods, such as chemical etching [31,32] and sol–gel synthesis [33,34], often generate a considerable amount of environmentally unfriendly wastewater and have long processing cycles, making them unsuitable for large-scale production. Compared with the aforementioned methods, the glass molding process (GMP) emerges as a convenient solution [35–37]. However, widely used precursor templates for glass molding, such as tungsten carbide and silicon carbide, pose issues for micro- and nano-fabrication due to their hardness and brittleness [38,39].

In this study, using a GMP-based strategy, we innovatively utilized soluble NaCl particles as precursor templates [40] to fabricate customizable porous structures on glass surfaces. By tuning the size and arrangement of the NaCl particles [41,42], multistage and size-tunable porous glasses were prepared, exhibiting continuous modulation in the range of superhydrophilicity (1°) to superhydrophobicity (142°). Notably, the outstanding oleophilicity demonstrated by the prepared porous glass surface endows it with extensive application prospects in the fields of oil–water separation and marine cleaning. Remarkably, thanks to the reversible nature of the changes in the glass's physical properties [43,44], the hydrophobic–oleophilic functionality of the glass surface remains preserved even after undergoing 10 repetitions of the manufacturing process. This demonstration highlights the convenience and cost-effectiveness of the strategy proposed for realizing special functionalities in glass. The introduction of a porous structure in glass reduces its transparency (Fig. S1), making it favorable for applications where privacy is emphasized. Therefore, superhydrophobic porous glass can be an ideal choice for use in bathrooms, conference rooms, and the construction industry. The results of this work provide a rapid and cost-effective new strategy for fabricating porous glass, thereby broadening the utilization of functional glass surfaces across various domains, such as self-

State Key Laboratory of Radio Frequency Heterogeneous Integration, Shenzhen University, Shenzhen 518060, China
* Corresponding author (email: majiang@szu.edu.cn)

cleaning and antifouling [45,46].

EXPERIMENTAL SECTION

Materials and dissolvable templates

D-K59 optical glass (Ø5 mm, 4 mm thick, CDGM Glass Co., Ltd., China) was the material of choice, which has a glass transition temperature (T_g) of 770 K and a softening temperature (T_s) of 824 K. NaCl particles (Sinopharm Chemical Reagent Co., Ltd.) were ground and screened to obtain particles in sizes of 50–150 μm, which were subsequently dried and used as templates for multistage glasses.

In addition, recrystallization was used to obtain 5-μm particles. Briefly, a saturated aqueous NaCl (Sinopharm) solution was added to an ethanol solution under vigorous stirring for complete mixing and recrystallization. The re-precipitated NaCl particles were then collected and vacuum-dried in a desiccator, finally obtaining the 5-μm NaCl templates.

Dissolvable template strategy

The preparation strategy of porous glass involved the stacking of glass and NaCl particles in a designed mold with a central through-hole of 5-mm diameter, using the NaCl particles as a template, and then placing the mold in a vacuum heating chamber. When the vacuum in the chamber was below 1×10^{-3} Pa, the whole chamber started to heat up at a rate of 40 K min^{-1}. After the temperature increased to 870 K, a pressure of 150 MPa was applied to the material placed in the mold using an indenter and the pressure was held for 1 min at a loading rate of 0.02 mm s^{-1}. After cooling, the sample was removed from the chamber and placed in distilled water to remove the NaCl template from the porous glass.

Multiscale structural characterization

The porous GMP was conducted with a self-developed machine (TM-YJ-03, Shenzhen University, China), which has a maximum heating temperature of 1470 K and load range of 0.2–30 kN and achieves an ultimate vacuum level as low as 3×10^{-4} Pa. Microscopic morphology of the porous glass was studied using an FEI Quanta 450 FEG scanning electron microscope (SEM). The surface microstructure of the porous glass was observed using a laser scanning confocal microscope (VK-

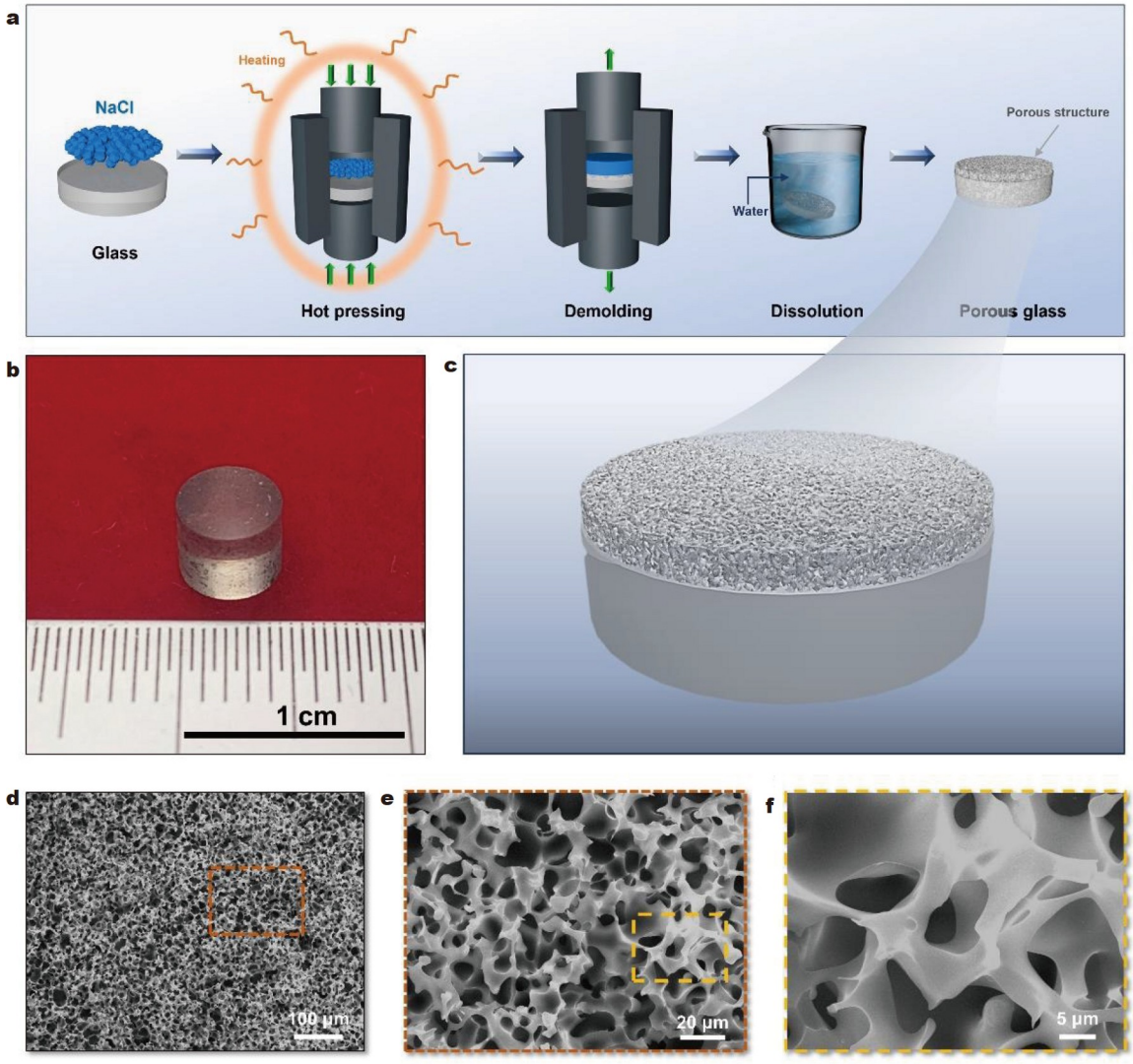

Figure 1 Characterizations of the prepared porous glass. (a) Schematic and (b) optical image of the manufactured porous glass; (c) schematic of the porous glass structure; (d–f) SEM images of the porous glass.

X250K, Keyence, Japan). Water contact angles were measured with a droplet shape analyzer (DSA100S, Krüss, Germany) with a droplet volume of 2 μL.

RESULTS AND DISCUSSION

Characterization of the porous MG

The procedure for the rapid preparation of porous glass is schematically illustrated in Fig. 1a. NaCl templates are stacked on the glass surface, and pressure is applied when the temperature of glass reaches the temperature region for that type of glass changes from solid to liquid, allowing the glass to completely fill the gaps between the templates. After cooling the sample and removing it from the heating oven, the sample was placed in distilled water at 343–373 K for 5 min to dissolve the template completely to obtain a porous glass. Fig. 1b illustrates the expeditious preparation of porous glass using the proposed method. Fig. 1c exhibits the schematic of the porous structure of this glass, while Fig. 1d–f show the microscopic morphology of its porous structure obtained using SEM. The multilayered porous structures spanning the glass surface serve to corroborate the scalability of the proposed method and its exceptional replication precision. The glass material exhibits outstanding fluidity within its softening temperature range, enabling it to seamlessly fill the interstices between NaCl particles when pressure is applied. Consequently, NaCl particles are fully encapsulated, and their subsequent dissolution results in the formation of the intricate pore-like structure shown in Fig. 1f.

Morphological design of porous structures

One notable advantage of using NaCl as a template lies in its capacity for facile size adjustment, which in turn allows facile tuning of the morphology and dimensions of the resulting porous structure. In this study, NaCl particles were prepared with diverse sizes, and the microscopic morphology of the resulting NaCl particles was examined by SEM, as illustrated in Fig. 2a_1–2a_3. Particle sizes were also counted. Results showed that recrystallization led to the smallest particles with an average size of 7.528 μm (Fig. 2b_1), while grinding followed by sieving yielded very large particles with an average size of 119.21 μm (Fig. 2b_2). Mixing large (with a uniform size distribution of 40–50 μm) and small (with a uniform size distribution of 5–15 μm) grain NaCl yielded particles with an average size of 19.841 μm (Fig. 2b_3). Using these NaCl particles of different sizes

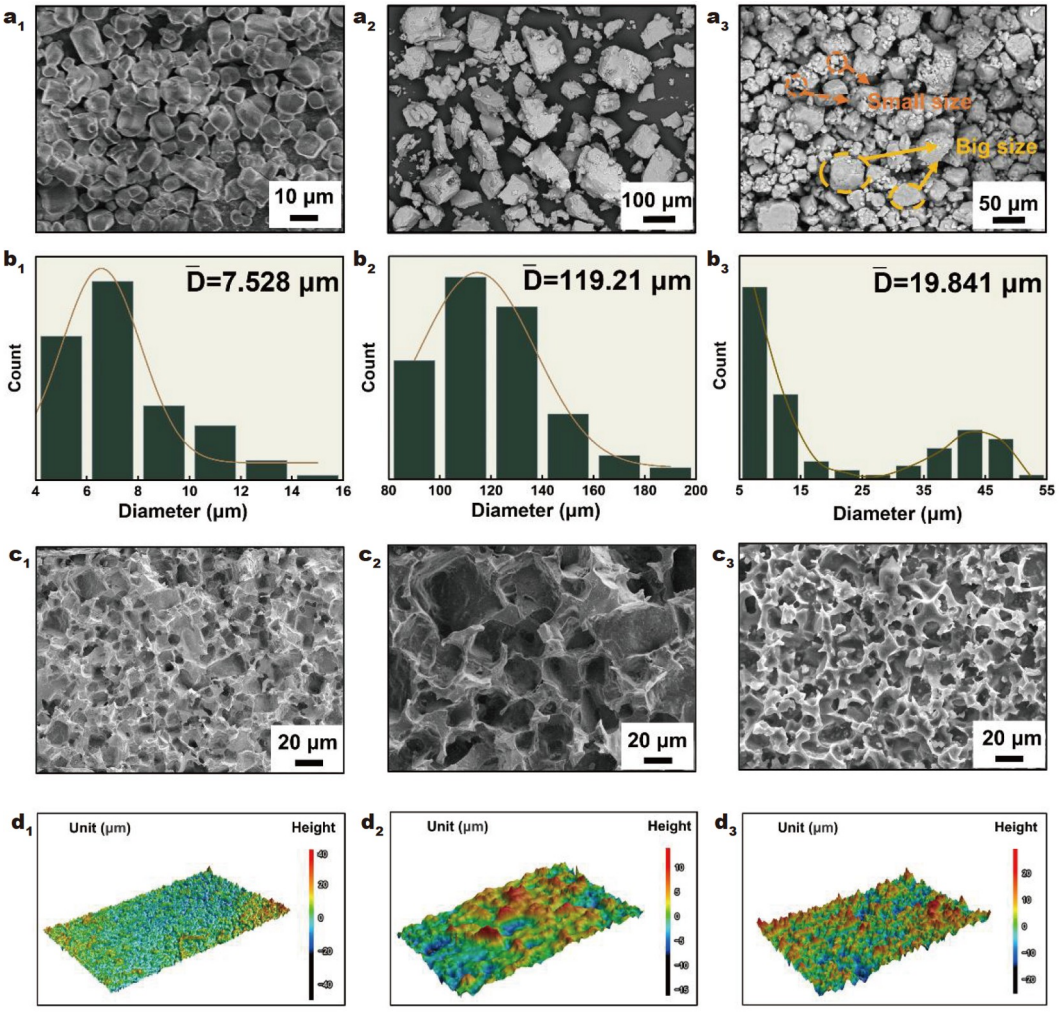

Figure 2 Characterizations of NaCl particles and porous glass. (a_1–a_3) SEM images of NaCl particles. (b_1–b_3) Particle size analysis images of salt particles in (a_1–a_3). (c_1–c_3) SEM images of the porous glass fabricated using different salt particles in (a_1–a_3). (d_1–d_3) 3D porous morphology of the glass porous structure of (c_1–c_3).

as templates, irregular porous structures on glass surfaces were realized (Fig. 2c$_1$–2c$_3$), which matched the size of the NaCl particles used. The hybrid particles produced porous structures with micro/nanocomposite structures (Fig. 2c$_3$) that closely replicated those on the NaCl template. The preparation strategy showed high replication accuracy and tunability, which was further confirmed by three-dimensional (3D) morphology analysis (Fig. 2d$_1$–2d$_3$).

Wettability of the porous glass

The water contact angle (WCA) and optimal contact angle (OCA) of the original optical glass are shown in Fig. 3a, b, respectively, demonstrating its surface wettability. The smooth surface of the unmodified glass has a stable WCA of approximately 50° (Fig. 3a) and an OCA of approximately 30° (Fig. 3b). The surface microstructure of a material affects its roughness and wettability. Fig. 3c, d present the porous structure on the glass surface, comprising numerous microscale pore-like and nanoscale pinning-like structures. Microstructure manipulation is an invaluable approach for changing the surface hydrophilicity of materials. In particular, the micro- and nano-composite structures in Fig. 3d represent a significant breakthrough in reducing the innate hydrophilicity of glass materials and considerably increasing their surface hydrophobicity. When liquid droplets come in contact with the intricate multilevel architecture on the material surface, air becomes trapped within the porous structure, leading to the formation of the gas cavity [47]. Consequently, droplets can find support from the dendritic nanoneedle structures shown in Fig. S2b, facilitating their further infiltration into the porous structure. In this case, the Cassie–Baxter equation [48] can be employed to explain the changes in the WCA of the porous glass.

$$\cos\theta_r = f_S\cos\theta - (1 - f_S), \quad (1)$$

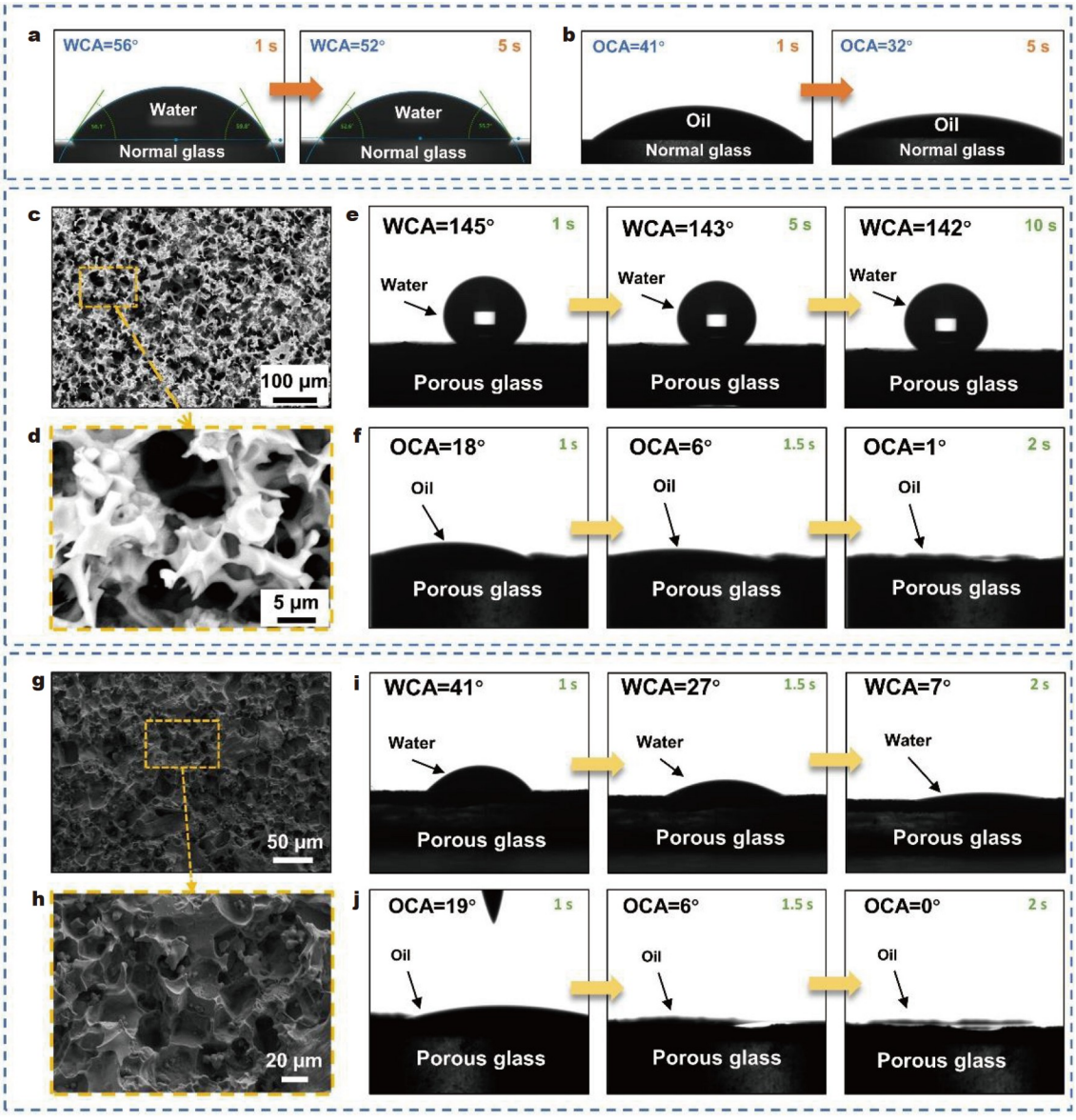

Figure 3 (a, b) WCA and OCA values of normal glass, respectively. (c, d) SEM images of porous glass with superhydrophobic and lipophilic properties. (e) WCA values of the porous glass at 1, 5, and 10 s. (f) OCA values of the porous glass at 1, 1.5, and 2 s. (g, h) SEM images of the porous glass with superhydrophilic and superlipophilic properties. (i) WCA values of the porous glass at 1, 1.5, and 2 s. (j) OCA values of the porous glass at 1, 1.5, and 2 s.

where θ_r is the WCA of the porous glass, f_S is the fraction of the solid–liquid interface, and θ is the WCA of the normal glass surface. Using this equation, f_S is found to be approximately 0.112, much smaller than 1. This finding reveals that when a water droplet encounters a superhydrophobic glass surface, approximately 88.8% of the contact areas are occupied by air, which is responsible for the excellent superhydrophobic property shown by the surface. Moreover, the introduced porous structure induces a remarkable change in the lipophilicity of the glass surface. This phenomenon can be explained using the Wenzel model [49], which posits that the porous structure not only modifies the surface roughness but also provides increased capacious interstitial regions for the liquid to penetrate, thereby improving the lipophilicity of the glass surface. Mathematically,

$$\cos\theta^* = r\cos\theta_y, \quad (2)$$

where θ^* is the OCA of porous glass, r is the roughness factor, and θ_y is the OCA of the normal glass. This micro/nanocomposite structure improves the hydrophobicity and lipophilicity of the material surface. Fig. 3e, f illustrate the process of contact angle change. The WCA remains stable above 140°, demonstrating excellent hydrophobicity, while the OCA rapidly approaches 0° in a short time, demonstrating exceptional lipophilicity. The porous structure shown in Fig. 3e, f endows hydrophilic and oleophilic properties to the glass surface with a WCA of less than 10° (Fig. 3i) and an OCA close to 0° (Fig. 3j). This porous structure has a larger pore size than the hydrophobic porous glass (Fig. 3c), with numerous micron-scale pores and no nanoscale structure, and it is this structure that allows water droplets to fully wet the glass surface and show hydrophilic properties [50]. Furthermore, rolling angle experiments were performed on the glass surface. Surprisingly, even when the sample was rotated 90° to a vertical position shown in Fig. S3, the water droplet remained intact, demonstrating excellent adhesion properties. The interplay of the inherent hydrophilicity of the glass material and the introduction of micro/nanocomposite structures on the material surface is responsible for its exceptional superhydrophobicity. Negative pressure caused by

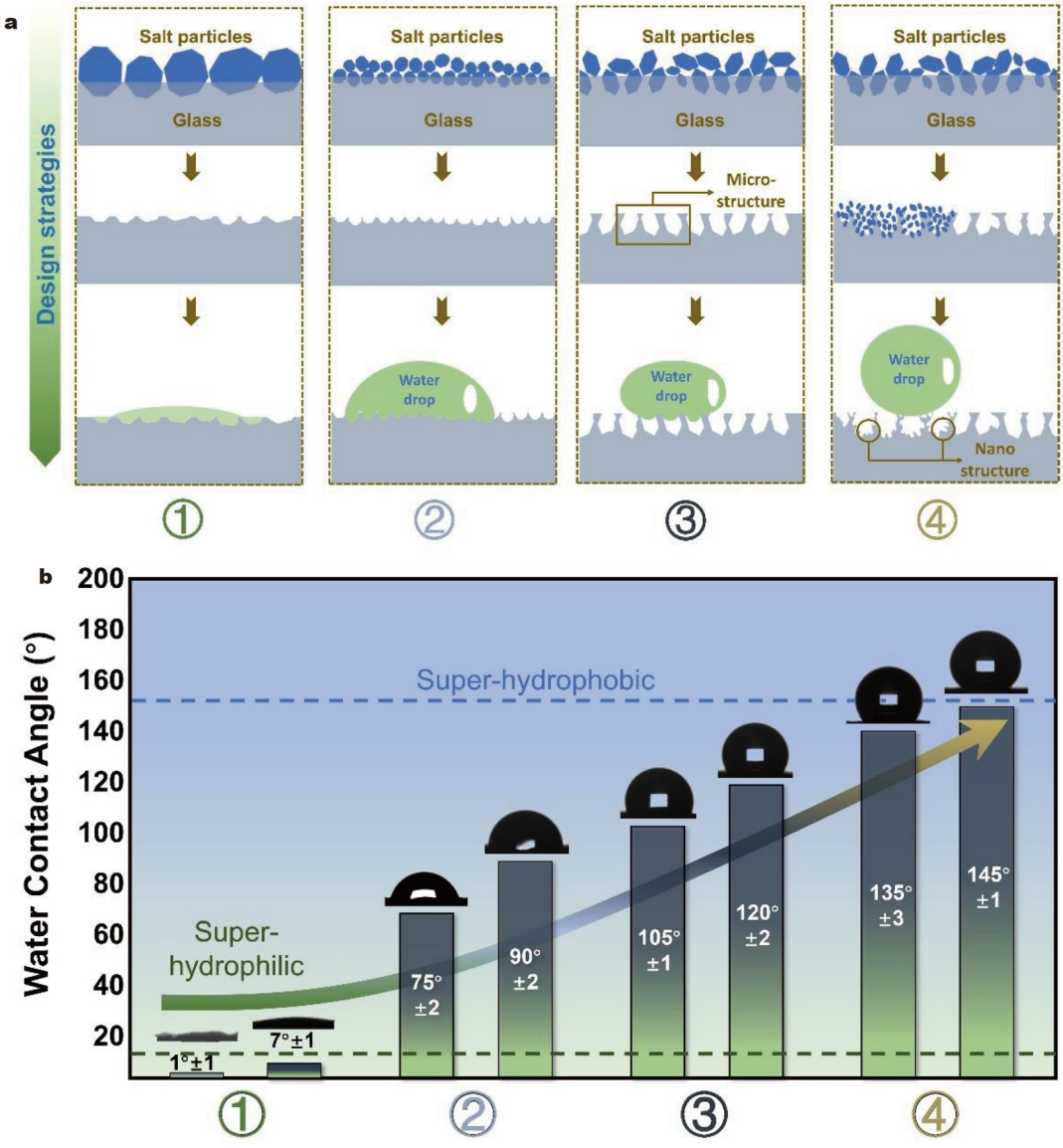

Figure 4 (a) Design strategies of the porous glass with multistage wettability; (b) WCA values of the porous glass prepared using different design strategies.

the volume change of the gas cavity and the van der Waals force [51] at the solid–liquid interface synergistically increase water droplet adhesion to a great extent. A wide range of self-cleaning applications can benefit from the superhydrophilic or superhydrophobic properties of porous glasses [52–54].

Multistage regulation design of the WCA of porous glass

The thermoplastic forming process is a convenient approach for producing porous structures on glass surfaces. By varying the experimental parameters, a multistage control for the WCA of the resultant porous glasses can be realized. As shown in Fig. 4a, four design strategies were used to regulate the glass surface wettability from superhydrophilic to superhydrophobic, all of which are based on thermoplastic formation and mainly involve tuning the NaCl particle size. The first strategy involves depositing very large NaCl particles (particle size > 100 μm) onto the glass surface, the second strategy uses 20–50 μm NaCl particles, the third strategy utilizes 50–100 μm NaCl particles, and the fourth strategy employs microfine NaCl particles obtained *via* recrystallization from 50–100 μm NaCl particles for a secondary thermoplastic forming process. The fourth strategy aims to produce more nanoneedle structures (Fig. S4), thereby increasing the glass's WCA. The implementation of these four distinct preparation strategies produced a diverse array of porous structures with varying sizes. The first strategy of using large-sized NaCl particles successfully engendered micromountain structures that spanned considerably across the glass surface. These structures have shallow cavities that effectively facilitate water infiltration, thereby profoundly amplifying the hydrophilic nature of the surface. In contrast, application of the second strategy resulted in densely packed micromountain structures capable of producing gas pockets below liquid droplets, unequivocally presenting their hydrophobic characteristics. With the objective of further improving the gas pocket effect, the

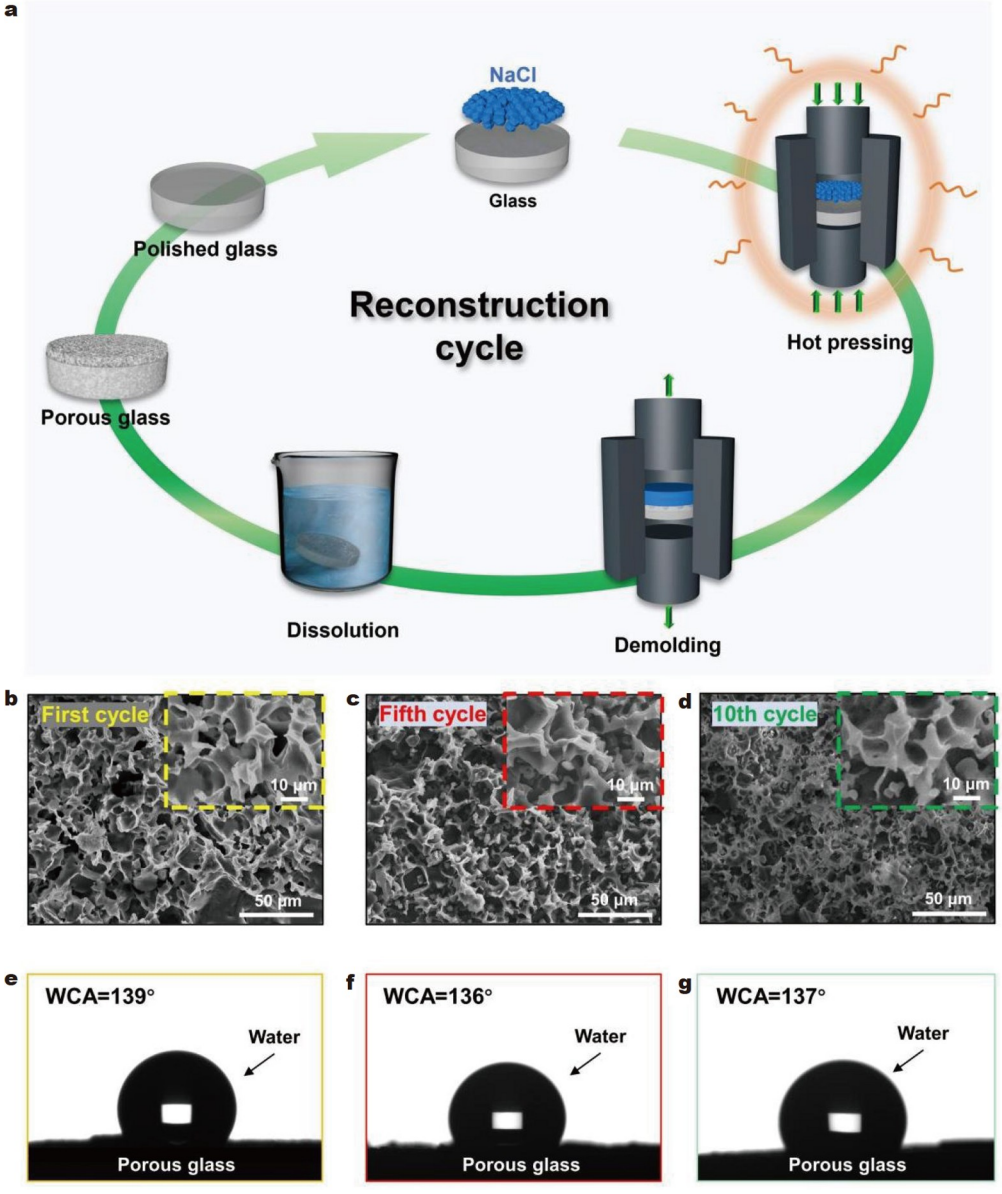

Figure 5 (a) Reconstruction of the porous glass. (b–d) SEM images of the porous glass fabricated in the first, fifth, and tenth cycles, respectively; (e–g) WCA values of the porous glass fabricated in the first, fifth, and tenth cycles, respectively.

third strategy focused on increasing the depth of the porous structures. The fourth strategy encompassed the integration of supplementary surface nanoprotrusions onto the existing porous structure, furnishing augmented storage capacity for air and exuding improved support for liquid droplets.

Fig. 4b illustrates the WCA values of the porous glasses prepared using these four strategies. The results vividly highlight the change in wettability of the glass surface from superhydrophilic to superhydrophobic. The NaCl dissolution fabrication strategy not only allows the generation of porous structures on glass surfaces but also facilitates the modulation of the template size, thus paving the way for preparing multifunctional glass surfaces.

Reconstruction of porous glass

Repeated use of porous glasses can cause structural damage to them, thereby affecting their performance; hence, investigating their reproducible preparation is crucial. Fig. 5a demonstrates a scheme showing the repetitive preparation of porous glass. When the porous structure on the glass surface is damaged, the damaged surface can be erased, and the porous structure can be re-prepared on the surface *via* the same preparation method. After reconstituting the glass surface several times, the samples corresponding to the first, fifth, and tenth cycles were characterized. Fig. 5b–d illustrate the surface morphology of the porous glass prepared in the first, fifth, and tenth cycles, respectively, along with their magnified images. Wettability tests were conducted, and the results revealed that all these samples maintained their WCA values above 135°, indicating that the reconstructed surface continues its good performance and confirming the feasibility of multiple reconstructions of porous glasses using this method.

CONCLUSION

In this work, porous glasses were successfully prepared using a soluble template strategy, imparting excellent hydrophobic and lipophilic properties to the glass surface. Various combinations of salt particles with varying sizes were employed to fabricate a range of irregular porous structures on the glass surface, enabling the precise regulation of the WCA values across multiple levels, spanning from superhydrophilic to superhydrophobic. This displays the inherent tunability and advantage of the preparation strategy proposed in this work. Additionally, the reversible nature of the physical changes observed in the glass material allows repeated construction of porous structures on its surface. Our preparation strategy overcomes the hard and brittle nature of glass materials, which pose problems to traditional manufacturing techniques, and enables the rapid preparation of micro- and nano-structures on glass surfaces. Meanwhile, the method presents a novel concept for preparing porous glasses, which can be widely used in various fields.

Received 4 September 2023; accepted 17 October 2023; published online 26 October 2023

1 Maeder T. Review of Bi_2O_3 based glasses for electronics and related applications. Int Mater Rev, 2013, 58: 3–40
2 Cai G, Wang J, Lee PS. Next-generation multifunctional electrochromic devices. Acc Chem Res, 2016, 49: 1469–1476
3 Ferdous W, Manalo A, Siddique R, *et al.* Recycling of landfill wastes (tyres, plastics and glass) in construction—A review on global waste generation, performance, application and future opportunities. Res Conserv Recycl, 2021, 173: 105745
4 Xiao Z, Liang S, Wang J, *et al.* Use of general regression neural networks for generating the GLASS leaf area index product from time-series MODIS surface reflectance. IEEE Trans Geosci Remote Sens, 2014, 52: 209–223
5 Wu T, Wu Z, He Y, *et al.* Femtosecond laser textured porous nanowire structured glass for enhanced thermal imaging. Chin Opt Lett, 2022, 20: 033801
6 Zhai M, Zhang S, Sui J, *et al.* Solid–solid phase transition of tris(hydroxymethyl)aminomethane in nanopores of silica gel and porous glass for thermal energy storage. J Therm Anal Calorim, 2017, 129: 957–964
7 Li H, Li J, Hou C, *et al.* Solution-processed porous tungsten molybdenum oxide electrodes for energy storage smart windows. Adv Mater Technol, 2017, 2: 1700047
8 Sun MH, Huang SZ, Chen LH, *et al.* Applications of hierarchically structured porous materials from energy storage and conversion, catalysis, photocatalysis, adsorption, separation, and sensing to biomedicine. Chem Soc Rev, 2016, 45: 3479–3563
9 Ren S, Zou W, Sun W, *et al.* Manufacturing and semi-analytical modeling of environment-friendly sound absorbent porous glasses. Appl Acoustics, 2022, 185: 108444
10 Fang Y, Zhang X, Zhou J. Experiments on reflection and transmission of acoustic porous metasurface with composite structure. Composite Struct, 2018, 185: 508–514
11 Liang C, Wang Z. Eggplant-derived SiC aerogels with high-performance electromagnetic wave absorption and thermal insulation properties. Chem Eng J, 2019, 373: 598–605
12 He YL, Xie T. Advances of thermal conductivity models of nanoscale silica aerogel insulation material. Appl Therm Eng, 2015, 81: 28–50
13 Zhang H, Zhang G, Gao Q, *et al.* Multifunctional microcellular PVDF/Ni-chains composite foams with enhanced electromagnetic interference shielding and superior thermal insulation performance. Chem Eng J, 2020, 379: 122304
14 Li Z, Wang B, Qin X, *et al.* Superhydrophobic/superoleophilic polycarbonate/carbon nanotubes porous monolith for selective oil adsorption from water. ACS Sustain Chem Eng, 2018, 6: 13747–13755
15 Wu Y, Weckhuysen BM. Separation and purification of hydrocarbons with porous materials. Angew Chem Int Ed, 2021, 60: 18930–18949
16 Zhu L, Shen D, Luo KH. A critical review on VOCs adsorption by different porous materials: Species, mechanisms and modification methods. J Hazard Mater, 2020, 389: 122102
17 Shen C, Wang YJ, Xu JH, *et al.* Porous glass beads as a new adsorbent to remove sulfur-containing compounds. Green Chem, 2012, 14: 1009
18 Chen YZ, Zhang R, Jiao L, *et al.* Metal-organic framework-derived porous materials for catalysis. Coord Chem Rev, 2018, 362: 1–23
19 Liang J, Liang Z, Zou R, *et al.* Heterogeneous catalysis in zeolites, mesoporous silica, and metal-organic frameworks. Adv Mater, 2017, 29: 1701139
20 Zhang G, Li Y, Xiao X, *et al. In situ* anchoring polymetallic phosphide nanoparticles within porous Prussian blue analogue nanocages for boosting oxygen evolution catalysis. Nano Lett, 2021, 21: 3016–3025
21 Zhou Y, Lohan DJ, Zhou F, *et al.* Inverse design of microreactor flow fields through anisotropic porous media optimization and dehomogenization. Chem Eng J, 2022, 435: 134587
22 Zheng T, Zhou W, Li X, *et al.* Structural design of self-thermal methanol steam reforming microreactor with porous combustion reaction support for hydrogen production. Int J Hydrogen Energy, 2020, 45: 22437–22447
23 Wang Y, Jin H, Ma Q, *et al.* A MOF glass membrane for gas separation. Angew Chem Int Ed, 2020, 59: 4365–4369
24 Jones JR. Review of bioactive glass: From Hench to hybrids. Acta Biomater, 2013, 9: 4457–4486
25 Chen ST, Jiang ZH. A force controlled grinding-milling technique for quartz-glass micromachining. J Mater Proc Tech, 2015, 216: 206–215
26 Ab Karim MS, Aly Diaa Mohammed Sarhan A, Hamdi Abd Shukor M. Experimental study on minimizing edge chipping in glass milling operation using an internal CBN grinding tool. Mater Manufact Proc, 2011, 26: 969–976
27 Zimmer K. Etching of fused silica and glass with excimer laser at 351

nm. Appl Surf Sci, 2003, 208-209: 199–204
28 Zhao J, Sullivan J, Bennett TD. Wet etching study of silica glass after CW CO_2 laser treatment. Appl Surf Sci, 2004, 225: 250–255
29 Nebiki T, Sekiba D, Yonemura H, *et al.* Taper angle dependence of the focusing effect of high energy heavy ion beams by glass capillaries. Nucl Instrum Methods Phys Res Sect B-Beam Interact Mater Atoms, 2008, 266: 1324–1327
30 Youn SW, Takahashi M, Goto H, *et al.* Fabrication of micro-mold for glass embossing using focused ion beam, femto-second laser, eximer laser and dicing techniques. J Mater Proc Tech, 2007, 187-188: 326–330
31 Enomoto I, Benino Y, Fujiwara T, *et al.* Synthesis of nanocrystals in $KNb(Ge,Si)O_5$ glasses and chemical etching of nanocrystallized glass fibers. J Solid State Chem, 2006, 179: 1821–1829
32 Kamenskii AN, Reduto IV, Petrikov VD, *et al.* Effective diffraction gratings *via* acidic etching of thermally poled glass. Opt Mater, 2016, 62: 250–254
33 Horváth M, Sinkó K. Hierarchical porous SiO_2 cryogel *via* sol-gel process. Gels, 2022, 8: 808
34 Zheng K, Boccaccini AR. Sol-gel processing of bioactive glass nanoparticles: A review. Adv Colloid Interface Sci, 2017, 249: 363–373
35 Tsai YC, Hung C, Hung JC. Glass material model for the forming stage of the glass molding process. J Mater Proc Tech, 2008, 201: 751–754
36 Li H, He P, Yu J, *et al.* Localized rapid heating process for precision chalcogenide glass molding. Opt Lasers Eng, 2015, 73: 62–68
37 Sun F, Yang J, Fu J, *et al.* Hierarchical macro to nano press molding of optical glasses by using metallic glasses. J Non-Cryst Solids, 2022, 594: 121821
38 Li K, Xu G, Wen X, *et al.* High-temperature friction behavior of amorphous carbon coating in glass molding process. Friction, 2020, 9: 1648–1659
39 Fischbach KD, Georgiadis K, Wang F, *et al.* Investigation of the effects of process parameters on the glass-to-mold sticking force during precision glass molding. Surf Coatings Tech, 2010, 205: 312–319
40 Huang J, Fu J, Li L, *et al.* Mg-based metallic glass nanowires with excellent photothermal effect. Scripta Mater, 2023, 222: 115036
41 Fu J, Li Z, Liu Z, *et al.* Manufacture of porous metallic glass using dissolvable templates. Sci China Mater, 2022, 65: 2833–2841
42 Liang X, Liu Z, Fu J, *et al.* Dissolvable templates to prepare Pt-based porous metallic glass for the oxygen reduction reaction. Nanoscale, 2023, 15: 6802–6811
43 Bauchy M, Micoulaut M. Densified network glasses and liquids with thermodynamically reversible and structurally adaptive behaviour. Nat Commun, 2015, 6: 6398
44 Jiang ZH, Zhang QY. The formation of glass: A quantitative perspective. Sci China Mater, 2015, 58: 378–425
45 Zhao Y, Xu T, Hu JM. A robust, room-temperature curable and molecular-level superhydrophobic coating with excellent antibacterial and antifouling properties. Chem Eng J, 2022, 450: 136557
46 Liu W, Kappl M, Butt HJ. Tuning the porosity of supraparticles. ACS Nano, 2019, 13: 13949–13956
47 Zhang W, Wang D, Sun Z, *et al.* Robust superhydrophobicity: Mechanisms and strategies. Chem Soc Rev, 2021, 50: 4031–4061
48 Cassie ABD, Baxter S. Wettability of porous surfaces. Trans Faraday Soc, 1944, 40: 546–551
49 Wenzel RN. Resistance of solid surfaces to wetting by water. Ind Eng Chem, 1936, 28: 988–994
50 Yan H, Yuanhao W, Hongxing Y. TEOS/silane coupling agent composed double layers structure: A novel super-hydrophilic coating with controllable water contact angle value. Appl Energy, 2017, 185: 2209–2216
51 Peng F, Wang D, Ma X, *et al.* "Petal effect"-inspired superhydrophobic and highly adhesive coating on magnesium with enhanced corrosion resistance and biocompatibility. Sci China Mater, 2017, 61: 629–642
52 Siddiqui AR, Li W, Wang F, *et al.* One-step fabrication of transparent superhydrophobic surface. Appl Surf Sci, 2021, 542: 148534
53 Zhang C, Xie H, Du Y, *et al.* Shelter forest inspired superhydrophobic flame-retardant composite with root-soil interlocked micro/nano-structure enhanced mechanical, physical, and chemical durability. Adv Funct Mater, 2023, 33: 2213398
54 Liu P, Lai H, Xia Q, *et al.* A shape memory porous sponge with tunability in both surface wettability and pore size for smart molecule release. Sci China Mater, 2021, 64: 2337–2347

Acknowledgements This work was financially supported by the Key Basic and Applied Research Program of Guangdong Province, China (2019B030302010), the National Key Research and Development Program of China (2018YFA0703605), the National Science Foundation of China (52122105 and 51971150), and the Science and Technology Innovation Commission Shenzhen (RCJC20221008092730037 and 20220804091920001). The authors also thank the assistance in microscopy observation received from the Electron Microscope Center of Shenzhen University.

Author contributions Liu J, Sun F and Ma J conceived the idea. Ma J, Ruan W, Ren S, Sun F, and Fu J supervised this work. Liu J carried out the experiments, designed and completed the experimental setup. Yu X, Zhang H and Wang W prepared the raw material for the experiment. Huang J and Zhu L performed the SEM. Liu J, Sun F and Ma J wrote the manuscript. All authors contributed to the discussion and analysis of the results.

Conflict of interest The authors declare that they have no conflict of interest.

Supplementary information Supporting data are available in the online version of the paper.

Junsheng Liu received his BSc degree from the South China Agricultural University in 2022. Currently, he is pursuing a Master degree in mechanical engineering at Shenzhen University. His research interest includes the formation of micro/nano-structure through thermoplastic forming process.

Jiang Ma received his BSc degree in materials science and engineering from the Southeast University in 2009 and PhD degree from the Institute of Physics, Chinese Academy of Sciences (CAS), Beijing, China, in 2014. He is currently a professor at the College of Mechatronics and Control Engineering, Shenzhen University, China, and received the Outstanding Teacher Award of Shenzhen, in 2018. His research interest includes the formation, functional application and high-frequency dynamic loading behavior of metallic glasses.

可定制多孔玻璃表面的溶解制造策略

刘俊升, 孙飞, 喻向阳, 张贺亭, 黄金标, 王文学, 朱立兴, 傅佳男, 阮文清, 任帅, 马将*

摘要 玻璃表面微纳结构的设计和制造在实现所需功能方面具有重要意义. 然而, 玻璃固有的硬度和脆性给传统制造方法带来了不便. 因此, 开发一种简单且可控的制造策略对于制备具备功能应用的微纳结构玻璃至关重要. 在本文中, 我们提出了一种创新方法, 利用可溶性氯化钠颗粒作为前驱体模板, 在玻璃表面上创建可定制的多孔结构. 通过我们的先导成型策略, 成功利用可溶性氯化钠颗粒的潜力作为前驱体模板, 从而便于制造量身定制的多孔玻璃表面. 通过调节这些颗粒的大小和组合, 我们实现了对所得多孔玻璃的连续调控, 范围从超亲水(1°)到超疏水(142°). 值得注意的是, 制备的多孔玻璃表面表现出显著的亲油性, 展示了在油水分离和自清洁等多种应用方面的巨大潜力. 最重要的是, 即使经过了10次制造迭代, 玻璃表面的疏水-亲油功能依然完好, 凸显了我们策略的耐久性和可重复性. 这种方法为实现玻璃的特殊功能提供了方便且具有成本效益的途径, 为不同领域的进展铺平了道路.

